ISSN 2354-9114 (online), ISSN 0024-9521 (print)
Indonesian Journal of Geography Vol 57, No.3 (2025): 637-648
DOI: 10.22146/ijg.105896 website: https://jurnal.ugm.ac.id/ijg

INDONESIAN JOURNAL OF GEOGRAPHY

RESEARCH ARTICLE

Soil Infiltration Rate at the Base of Karst Valley in the Gunungsewu Karst, Indonesia

Eko Budiyanto[1*], Nugroho Hari Purnomo[2], Insan Wastuwidya Mahardiani[2], Eko Haryono[3]

[1]Geography Education Department, Universitas Negeri Yogyakarta, Indonesia
[2]Geography Education Department , Universitas Negeri Surabaya, Indonesia
[3]Faculty of Geography, Universitas Gadjah Mada, Indonesia

Received: 2025-04-10
Revised: 2025-10-10
Accepted: 2025-12-16
Published: 2025-12-31

Key words: Soil infiltration rate; Horton model; Gunungsewu karst

Correspondent email: ekobudiyanto@uny.ac.id

Abstract. The Gunungsewu Karst is a landscape that is highly vulnerable to degradation. Infiltration rate is a critical factor in efforts to protect and conserve karst environments, however, studies focusing specifically on infiltration processes at the valley floor of karst systems, particularly in relation to the morphological characteristics of the Gunungsewu karst, remain limited. This study aims to examine the characteristics of soil infiltration rates at the bottom of the Gunungsewu karst valleys based on their morphological units. Field measurements of infiltration rates were conducted using a double-ring infiltrometer, and infiltration parameters were calculated using the Horton model. Sampling was carried out according to the morphological classification of the Gunungsewu Karst, which includes rounded karst cone units (K1), elongated karst cone units (K2), and trapezoidal karst cone units (K3). Data analysis employed a descriptive approach based on data distribution, visualized using box-and-whisker plots and line graphs.The results indicate distinct differences in infiltration rate characteristics among the morphological units. Infiltration rates across all sites ranged from 0.10 cm min^{-1} to 0.65 cm min^{-1}. The highest infiltration rates were observed sequentially in the K1, K2, and K3 units. Variations in infiltration rate characteristics within the study area are strongly influenced by morphological features, lithology, vegetation cover, and land use. These findings enhance the understanding of infiltration rate characteristics in karst environments and provide a scientific basis for the development of sustainable strategies for karst environmental protection and conservation.

1. Introduction

Soil has a very important role in karst areas because it functions as a growing medium for plants and, at the same time, a pollutant filtration agent for groundwater (Hindersah et al., 2021; Liu et al., 2022). An important soil property to note for various analyses and technical importance is the infiltration rate (Béjar-pulido et al., 2021; Polyakov et al., 2020; Zhang et al., 2022; Zhang et al., 2025; Zou et al., 2025). The process of water infiltration in karst soil has been proven to be able to carry soil particles in the form of solutions or granules, which is the beginning of the erosion process (Hervé-Fernández et al., 2023; Zhang et al., 2024). Infiltration can also result in the transfer of mineral ions in karst soils either vertically or laterally (Luo, 2022; Zhang et al., 2022). Vegetation cover, land tillage, rock fragment, and soil moisture are key triggers for the level of infiltration in karst land (Li et al., 2011; Béjar-pulido et al., 2021; Dahak et al., 2022) .

The soil in the Gunungsewu karst area has been proven to have a lot of clay texture (Haryono, 2017). Soils with a clay texture tend to have a higher level of water-holding capacity (Li et al., 2022). This results in a lot of water being entangled by karst soil. Soil moisture persists for a relatively longer time, as water is strongly bound by soil particles. However, the presence of clay in karst soil can trigger high wrinkles. The higher the clay content in karst soil, the more likely the soil is to wrinkle when it meets water (Elhassan et al., 2023; Tong et al., 2021). The nature of soil wrinkles can cause difficulties in the use of soil on the land technically (Bala & Patel, 2023). The problem of land use is not only in the use related to buildings but also in maintaining soil fertility for agriculture. Meanwhile, land utilization has been intensively carried out for housing and agricultural activities.

The Gunungsewu karst landscape is formed on karst hills with several types of morphology that vary. Land form differentiation in the Gunungsewu karst is based on the interaction between bedrock, structural discontinuity, and subsurface hydrological processes, which further form three sub-types, namely labyrinth-cone, polygonal, and residual cone karst (Haryono & Day, 2004). Srijono, et al. (2018) provides a more detailed classification of the Gunungsewu karst landscape into five distinct geomorphic units, namely the rounded karst cone, the longitudinal karst cone, the trapezoidal karst cone, the karst marginal plain, and the dry valley. The three morphological classification units are consistent with the landform sub-types identified by Haryono and Day (2004),

The morphological evolution of the Gunungsewu karst is governed predominantly by variations in lithology and underlying geological structures (Kusumayudha et al., 2016). The Gunungsewu Karst is included in the lithological unit of the Wonosari Formation and has a regional slope to the south.

The Wonosari Formation consisting of two limestone outcrop features which are the result of karstification and calichification processes, consisting of four lithofasies, namely packstone, wackestone, boundstone, and marl (Kusumayudha et al., 1999). The facies are derived from closed carbonate exposure sedimentation environments that form packstones, and open marine platforms that form wackestone and boundstone (Aliyan et al., 2023). The facies are spread relatively north-south. The findings of the inconsistency of calichic with packstone, boundstone, and wackestone were used as the basis for estimating the carbonate age of Gunungsewu by Sutoyo (1994). Thus, sequentially, the bedrock in the northern part of the Gunungsewu karst has the oldest age marked by the presence of calichic and packstone, boundstone, and wackestone fasies. In accordance with this, Tjia (2013) also outlines that the age of the youngest rocks was on the south side parallel to the current coastline, and the age of the older rocks spread north. The morphological unit and age of the bedrock that forms the Gunungsewu karst landscape are interesting to study in relation to the rate of infiltration in the soils in the location.

Gunungkidul Regency is experiencing increasing population growth. The population of Gunungkidul Regency in 2020 was 747,160 people increasing to 753,190 people in 2025 with the population growth rate from that year being 0.17% (BPS, 2025). In line with its growing population, the Gunungsewu karst region has continued to undergo increasing land-use intensification (Sunkar, 2008; Reinhart et al., 2023), particularly on land situated at the base of karst valleys as an intesive agricultural land. Agricultural tillage activities have been proven to change the characteristics of soil infilation (Béjar-pulido et al., 2021). Agricultural land in karst valleys is extensively utilized for secondary crop cultivation, particularly during the rainy season (Budiyanto et al. 2023; Reinhart et al, 2023). The application of fertilizers and pesticides on rainfed paddy fields and dryland agricultural areas—both of which dominate land use within the recharge zone—contributes to the formation of potential pollution sources (Naufal et al., 2024). In line with the above conditions, the land in the Gunungsewu karst area urgently needs protection and preservation efforts.

Karst areas have the potential to serve as zones of groundwater infiltration, although the quantity of infiltration varies (Ashgaf et al., 2019). The level of soil infiltration in karst areas is very important, considering the rapid infiltration rate, which has proven to have a high potential for groundwater pollution (Sang et al., 2023; Steiakakis et al., 2023). The understanding of infiltration rate is used as the basis for soil conservation at each karst area site and also groundwater conservation (Dahak et al., 2022; Li et al., 2024). Variations in soil infiltration at the base of karst valleys are fundamental to technically defining appropriate land use (Liao et al., 2025). However, studies focusing specifically on infiltration processes at the valley floor of karst systems, particularly in relation to the morphological characteristics of the Gunungsewu karst, remain limited. This study aims to examine the characteristics of soil infiltration rates at the bottom of the Gunungsewu karst valley based on its morphological units in the context of an effort to protect and maintain the sustainability of the Gunungsewu karst environment.

2. Methods

This research was conducted in the karst valley in the Gunungsewu karst area which is included in the Gunungkidul Regency, Special Region of Yogyakarta Province as shown in Figure 1.

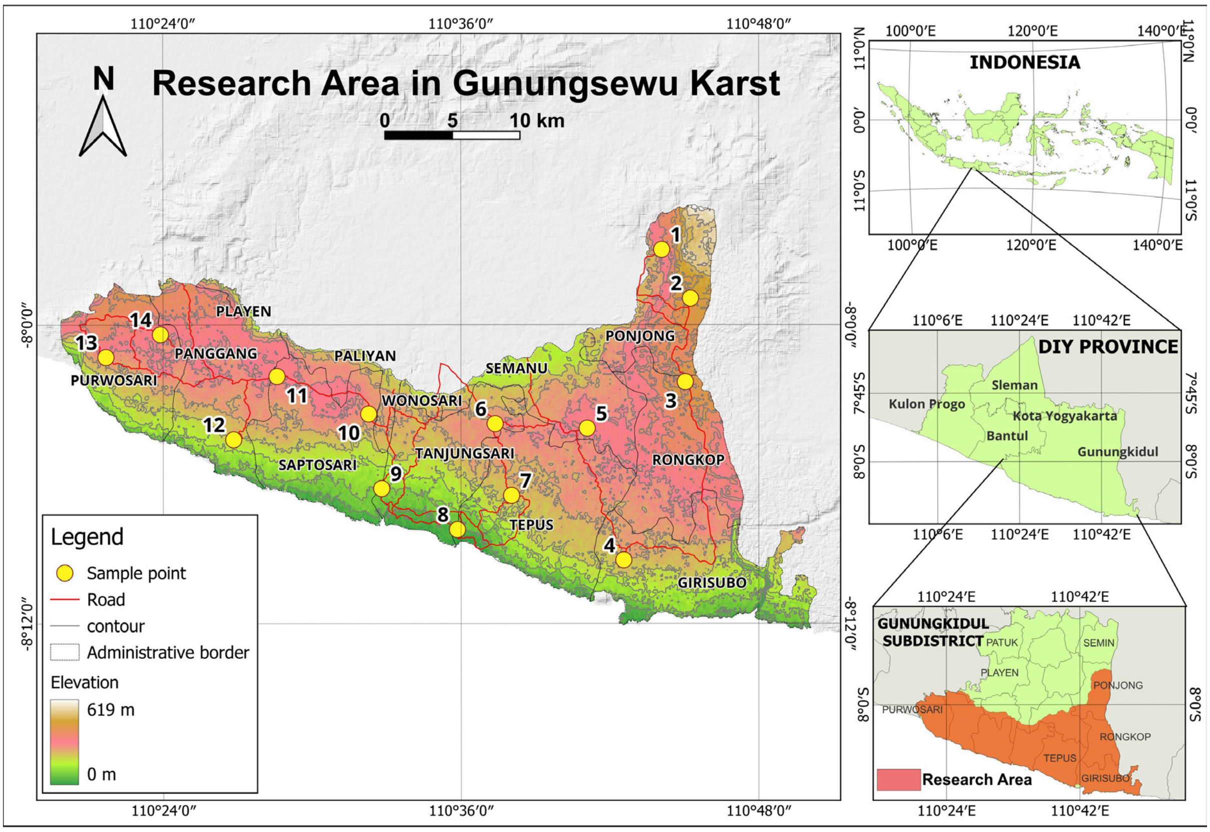

Figure 1. Infiltration measurement sample location

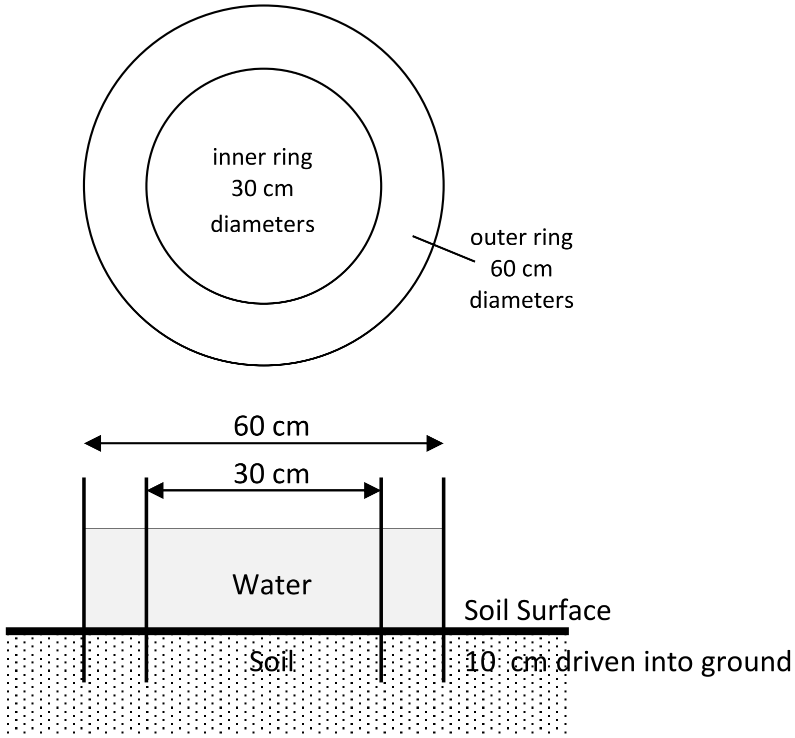

Figure 2. Infiltration measure with double-ring infiltrometer

Karst valleys were identified through DEM analysis from SRTM imagery data on the coordinate reference system EPSG: 32749, WGS 84/UTM Zone 49S. The distribution of karst valleys was derived from a closed-depression analysis performed using SAGA software. The results of this analysis provide information on the spatial patterns of valley sequences within the study area. These patterns of karst-valley distribution were subsequently used as a basis for interpreting the surface morphology of the karst landscape. The sample was determined by considering the morphological classification of the surface of the karst land submitted by Haryono and Day (2004) and Srijono et al. (2018). In each part of the morphological unit, samples were taken on the north and south sides of the Gunungsewu karst area in line with (Sutoyo, 1994). The total sample locations taken are as many as 14 locations spread across the southern and northern parts of the Gunungsewu karst.

The measurement of the infiltration rate at the sample location was carried out on the soil of the karst valley, which was flat and not vegetated. Measurements were made using a double-ring infiltrometer. The design of the use of a double-ring infiltrometer in the field is shown in Figure 2.

The size of the inner ring is 30 cm in diameter by 30 cm in height, while the outer ring is 60 cm in diameter with a height of 30 cm. On the inner ring wall is installed a ruler to read the water level.In the infiltration measurement process, the ring is installed with a depth of 5 cm to 10 cm in a flat position. Water is filled in the outer ring chamber to a height of 15 cm to 20 cm, and continued with water is filled in the inner ring chamber to the same height. The water in the outer ring chamber functions as a buffer to minimize the lateral movement of water in the inner ring chamber. The water level (h) in the inner ring chamber is recorded in a period (t) of 5 minutes. Recording is considered sufficient if the change in water level (Δh) has been stable up to 5 times the recording time. Infiltration capacity (f) is calculated by dividing the change in water level between times (Δh) by the observation time (t). Constant infiltration (fc) at the sample point is recorded when the infiltration capacity (f) value has stabilized up to five times the measurement. The infiltration rate modeling was carried out using Horton's equation based on the results of field measurements. The Horton equation used in this study is as follows.

$$I = fc + (f0 - fc)\, e^{-kt} \quad (1)$$

I is the infiltration rate, fc is the constant infiltration capacity level, $f0$ is the infiltration capacity at 0 minutes, k is the Horton coefficient, which depends on soil and vegetation conditions, and t is the infiltration process time.

Characterization of infiltration rates within each morphological unit was conducted by classifying infiltration-rate values according to the morphological units defined by Srijono et al. (2018). The Gunungsewu karst that is included in the research area consists of K1, K2, and K3 units. The grouping was derived from an overlay of the infiltration-measurement sample site map with the morphological-unit map of the western sector of the Southern Mountains. This overlay was performed using QGIS software. Based on the morphological unit map (Srijono et al., 2018), the observation location of this study is in rounded karst cone units (K1), elongated karst cone units (K2), and trapesoidal karst cone units (K3). Samples within the K1 unit comprised sample numbers 1, 2, 3, 4, 5, and 6, whereas samples within the K2 unit comprised sample numbers 7, 8, 9, and 10. Samples assigned to the K3 unit included sample numbers 11, 12, 13, and 14. The analysis of the box-whisker graph was used to determine the range of infiltration velocity, mean, lower quartiles, and upper quartiles. The morphological-unit map of the western sector of the Southern Mountains as shown in Figure 3.

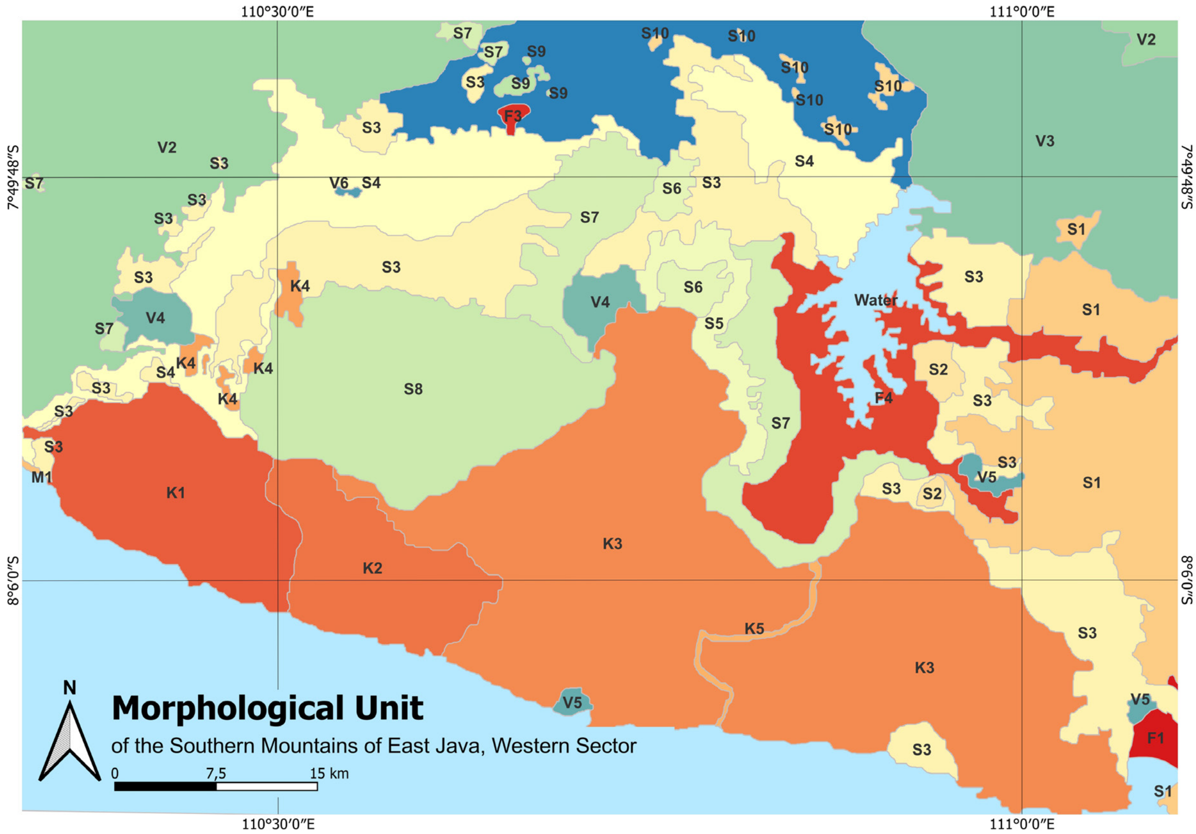

Figure 3. the morphological-unit map of the western sector of the Southern Mountains. Map source : Srijono et al. (2018).

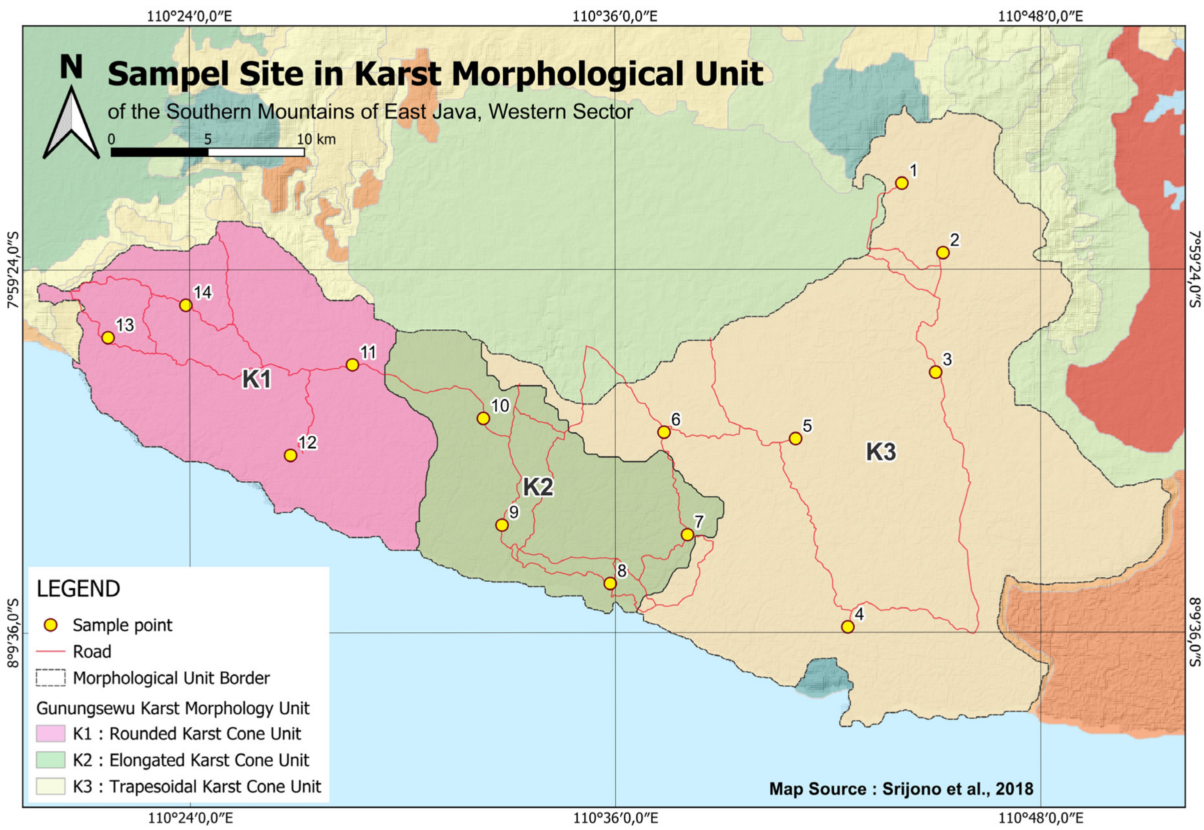

Figure 4. Sample site of the research in the karst morphological-unit. Map source : Srijono et al. (2018)

Infiltration characterization was also conducted based on the classification of sample locations into northern and southern sectors. This grouping was employed to examine differences in infiltration characteristics between the northern and southern parts of the Gunungsewu karst area. The southern sector included sample numbers 4, 7, 8, 9, 12, and 13, while the northern sector comprised sample numbers 1, 2, 3, 5, 6, 10, 11, and 14. The location of the sample in the karst morphological unit Srijono et al., (2018) is shown in Figure 4. The analysis was based on graphical representations of infiltration-rate values from both sectors. The infiltration-rate values within each morphological-unit group were subsequently plotted as box-and-whisker plots and line graphs, which served as the basis for analyzing the infiltration characteristics across the respective land units. The characterization of the infiltration rate on the north and south sides of the study area is based on box-whisker values consisting of the range of infiltration values, mean, lower quartiles, and upper quartiles. Line graphs are used to show the infiltration value ratio of each sample that has been sorted based on its location. Locations that are in a north-south position will appear on the graph on the same axis.

3. Results and Discussion

Karst valley conditions

The land at the bottom of the karst valley is used as agricultural land especially in the rainy season. During the dry season, a lot of land is not planted because of the harsh soil conditions and lack of water. This condition is in line with the findings of Reinhart et al. (2023) who describe that the development of land use into agricultural land in the Gunungsewu area is the largest compared to other uses. Clearing of agricultural land at the bottom of karst valleys is more intensive than land on hillsides that tend to have steep slopes. This agricultural activity has been proven to increase the ability of matrix infiltration in the soil (Liao et al., 2025), and changes in the composition of soil minerals such as Ca and Mg (Luo, 2022) which are key elements in karst rocks. The hillsides have many rock outcrops, thin soil thickness, and vegetation cover. The vegetation that grows is in the form of grass, shrubs, and woody plants with sparse density.

At the location of the sample that has such characteristics, the soil grains easily expand. The soil condition at the bottom of the Gunungsewu Karst Valley generally has hard properties, and there are many large, sturdy soils. The research was conducted in the dry season. The soil is sturdy up to 3 cm in size with a depth of approximately 10 cm. There are many grains from the destruction of soil aggregates on the surface. This is in line with the opinion of Widyastuti & Haryono, (2016) which explains that in the dry season the soil at the research site can crack up to more than 5 cm. When filling the ring with water, the cracks in the soil under the ring can quickly close. Infiltration can run vertically without leakage from the soil cracks but can cause preferential infiltration through gaps in the interior of the soil (Jiaxin et al., 2025; Liao et al., 2025; Wang et al., 2018). Preferential infiltration is a form of water infiltration through soil cavities formed by aggregate fragments or their contact with rock surfaces or roots. This condition is in line with the conclusion from Hu et al. (2021) who explain that agricultural activities trigger the formation of an argic horizon, which is an increase in clay content in the layer below the surface. This condition triggers higher wrinkles on the karst valley soil which can produce cracks on the ground surface. The condition of the bottom soil of the karst valley and slope as shown in Figure 5.

The picture is a condition that represents the condition of the soil on the south side of the Gunungsewu karst. The color of the soil in some locations is dark reddish brown, and in some locations it is dark brown. Some of the soil color of the Gunungsewu karst valley in this study is similar to the findings from Sitinjak et al. (2019) on karst soil in the Malang area. In line with these findings, Mulyanto et al. (2011) concluded that the Gunungsewu karst soil with red color is the result of intensive decalcification so that it has the characteristics of low pH, alkaline saturation, and Cation Exchange Capacity (CEC). Different conditions occur in black soils which are derivatives of clay containing navel after the dissolution of $CaCO_3$.

Infiltration Rate

Field infiltration measurements were successfully conducted using a double-ring infiltrometer and yielded variable results across the measurement locations. The measurement sites were generally situated on flat terrain at the bottom of karst valleys. The field infiltration measurement procedure is shown in Figure 6.

The measurement time between locations to achieve *fc* value up to 5 times is varied. Measurements were taken at each sample location with a duration of between 50 minutes to 100 minutes until a constant infiltration value was achieved 5 times. Data that is considered invalid is corrected by re-measuring the location. The location of the infiltration measurement sample spread on the south side of the study area relatively took

Figure 5. Soil conditions and slopes of karst valleys at sample 7th site.
Source : Field observation (2023)

Figure 6. Infiltration measurement process at sample 9th site.
Source: Field observation (2023)

Table 1. Infiltration capacity as a result of field measurements

Sample	***Fc***	
	(*cm/minute*)	(*mm/hour*)
1	0.40	240
2	0.10	60
3	0.30	180
4	0.55	330
5	0.30	180
6	0.10	60
7	0.35	210
8	0.45	270
9	0.30	180
10	0.10	60
11	0.40	240
12	0.65	390
13	0.45	270
14	0.26	156

Source : Field measurement (2023)

longer than the measurement on the north side. The repetition process is more carried out in this southern side sample area, so the measurement process requires more time and water. This condition occurs in the morphological units K1, K2, and K3. Most of the measurement processes in the three morphological units are relatively longer and there is a process of repetition of measurements. This condition is made possible by differences in lithology, type of cover vegetation, physical properties of the soil, and land use as shown by research conducted by X. Li et al. (2011), Lin et al. (2025), Gan et al. (2023), and Zeng et al. (2024). Lithology exerts an influence on the physical properties of the soil and the vegetation that develops at the site. Vegetation influences soil properties such as soil organic carbon, soil moisture, and increased infiltration through its root network system (Zhang et al., 2025). Land use can change the type of infiltration in the soil. The existence of such vegetation, especially woody trees, is very important in maintaining the level of infiltration. The results of infiltration measurements in the field using a double ring infiltrometer produce infiltration data as shown in Table 1.

The calculation using the Horton model for all sample locations yielded the values of *f0*, *fc*, *k*, and the basic infiltration value (*b*) of each location. Based on the r^2 value of Table 2, it can be stated that the Horton model has good accuracy and can be used to measure the infiltration rate on Gunungsewu karst soil. The results of the calculation using the Horton method can be used to predict the level of infiltration at a certain time after rain in the Gunungsewu karst area. The ability of the Horton model on the Gunungsewu karst soil is in line with Béjar-Pulido et al. (2021), who concluded the accuracy of the

Horton infiltration model on Andosol soil. The results of this calculation are also in accordance with the results of a study from Robin and Bora (2019), which concluded that the Horton model gives good results in hilly areas. Based on the r^2 value obtained, the accuracy of the measurement of the Horton method in this study ranges from 0.92 to 0.99 which means it has a narrower range than the measurement results from Robin and Bora (2019) but it is broader than Béjar-Pulido et al. (2021). The advantage of using this Horton model is that it is able to show the initial and final infiltration which is mainly influenced by the initial soil moisture conditions, land cover, and soil type (Dahak et al., 2022).

The difference in the infiltration characteristics of Gunungsewu karst soil is related to the value of initial infiltration (*f0*), infiltration capacity (*fc*), and the speed of achieving infiltration capacity constant. At all measurement locations, there was a drastic decrease in the rate of infiltration, and then it leveled off until it reached a constant condition.

The lowest *values of f0* and *fc* were found in sample number 2. The *f0* value is 0.47 cm/minute and *the fc* value is 0.1 cm/minute. The location of sample number 2 is agricultural land with a fairly large area and is included in the residual cone karst morphology unit (Haryono & Day, 2004). The highest *f0* and *fc* values occurred in sample 12. The *f0* value of the location is 3.42 cm/minute, and the *fc* is 0.66 cm/minute. The location is in the form of a valley extending to the beach with a steep slope. The measurements are in an elongated karst valley and are covered with relatively steep slopes. The land at the location is used as agricultural land with the type of crops being palawija. At the time of measurement, the land was empty because there was no water to irrigate the plants on the land. The infiltration characteristics in the Gunungsewu karst area can be depicted in the Horton model infiltration rate graph. Some infiltration rate graphs of field data and Horton models are shown in Figure 7.

Table 2. Horton model infiltration parameter value

Sample	*f0*		*fc*		*k*	*b*	r^2
	(cm/minute)	(mm/hour)	(cm/minute)	(mm/hour)			
1	1.24	744	0.40	240	-0.2652	-0.1797	0.99
2	0.47	282	0.10	60	-0.0738	-0.9898	0.92
3	1.27	762	0.33	198	-0.2282	-0.0333	0.99
4	1.48	888	0.62	372	-0.1276	-0.0769	0.96
5	0.71	426	0.32	192	-0.2118	-0.9025	0.86
6	0.60	360	0.11	66	-0.2761	-0.6931	0.85
7	1.53	918	0.37	222	-0.2360	0.1633	0.98
8	1.26	756	0.49	294	-0.1887	-0.2160	0.94
9	2.49	1494	0.35	210	-0.1602	0.7839	0.98
10	0.69	414	0.10	60	-0.1221	-0.5313	0.96
11	2.11	1266	0.43	258	-0.1789	0.5374	0.91
12	3.42	2052	0.66	396	-0.3369	1.0171	0.99
13	1.34	804	0.46	276	-0.3577	-0.1116	0.98
14	1.14	684	0.26	156	-0.1815	-0.1258	0.99

Source: Calculation results

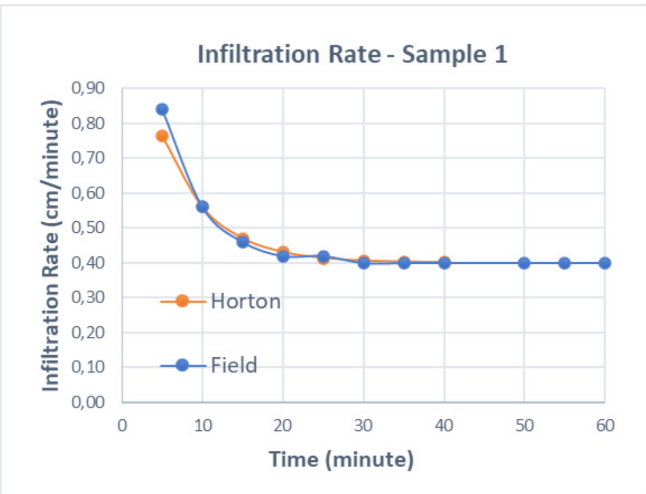

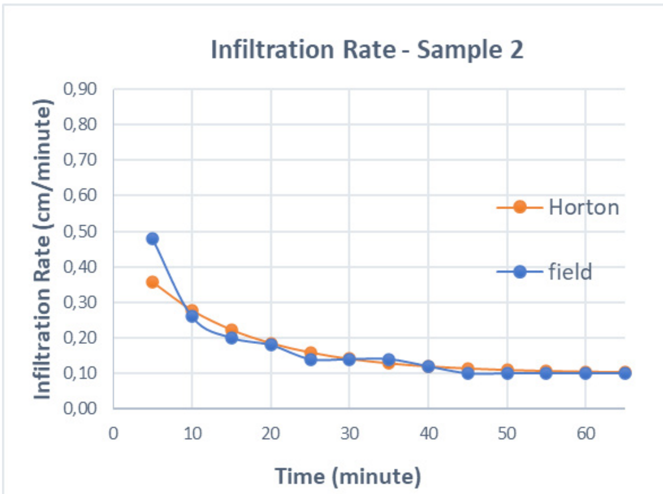

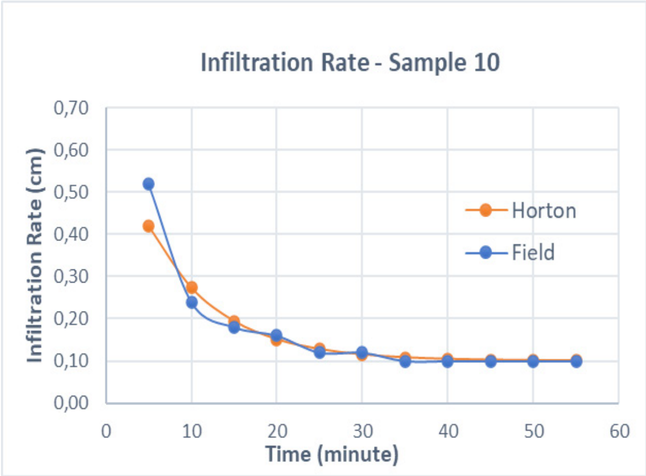

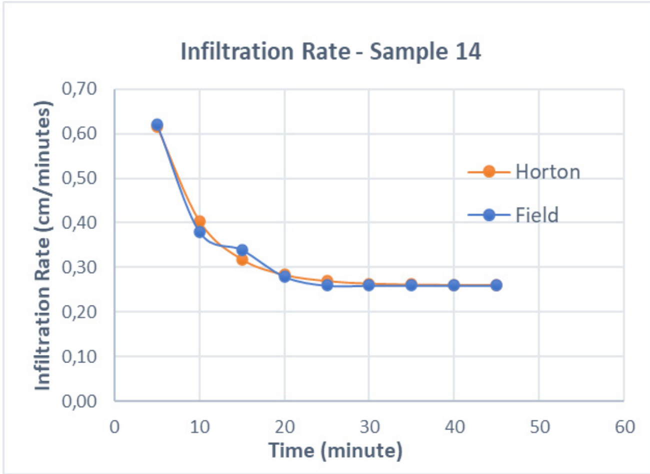

Figure 7. Infiltration Rate from Field Data and the Horton Model.
Source : Calculation result

The results of the analysis showed that there were differences in the characteristics of the infiltration rate in the morphological units of K1, K2, and K3. Based on the analysis of infiltration-rate distributions across the morphological units, the ranges of infiltration rates differ considerably. The box and whisker plot analysis of the infiltration rate data is shown in Figure 8.

The K1 unit exhibits infiltration-rate values that cluster closely around the mean. Field measurements indicated that the infiltration rate ranged from a minimum of 0.26 cm/min to a maximum of 0.65 cm/min, with an average value of 0.44 cm/min. The boxplot analysis further showed that the interquartile range extended from the lower quartile (0.37 cm/min) to the upper quartile (0.50 cm/min). Overall, the infiltration rate in the K1 area is the highest compared with those observed in the K2 and K3 morphological units, indicating a greater capacity of the soil in this area to transmit water.

According to the classification of Srijono et al. (2018), the K1 area corresponds to a rounded karst-cone unit, which aligns with Haryono and Day (2004), who describe it as polygonal karst. This morphological unit was formed through dissolution processes and the influence of southward-directed fluviation along the general slope of the area, resulting in a closed valley with slope gradients ranging from 15° to 31° in most parts and a weakly developed valley network (Haryono & Day, 2004). The K1 unit area, particularly its northern sector, exhibits denser woody vegetation cover than the K2 and K3 unit areas. Dense woody vegetation can enhance soil bulk density and improve soil physical properties thereby enhancing the soil's infiltration capacity (Gan et al., 2023; Hidayat et al., 2024; Li et al., 2011). Soil-rock interface have a significant role in increasing infiltration capacity when there is an increase in soil bulk density (Zhao et al., 2025). The increasing age of trees has been proven to increase the infiltration capacity of the soil below (Huang et al., 2024; Zhang et al., 2025). Therefore, the denser vegetation cover in the K1 unit is likely to promote higher infiltration rates compared to the other units.

The infiltration rate in the K2 area exhibits a lower overall distribution than that observed in the K1 area across most parameters. Nevertheless, the range of infiltration-rate values in K2 is comparable to that of K1. In the K2 unit, infiltration rates range from a minimum of 0.10 cm/min to a maximum of 0.45 cm/min, with a mean value of 0.30 cm/min. Box and whisker plot analysis indicates that the interquartile range extends from the lower quartile (0.25 cm/min) to the upper quartile (0.38 cm/min). These results demonstrate that the infiltration rate in the K2 morphological unit is generally lower than that in the K1 area.

The K2 morphological unit is in the form of elongated hilly morphology that generally extends northwest – southeast, and west-east on the southern side of the Gunungsewu karst (Srijono et al., 2018). Haryono & Day (2004) refers to it as a labyrinth-cone karst characterized by a series of valleys and elongated hills controlled by faults or major joints. The hillslopes in this area are generally steeper than those in the K1 and K3 units, resulting in relatively thin soils and abundant rock outcrops. Land at the bottom of the karst valleys is predominantly used by local communities for agriculture, settlements, and other activities. Vegetation density in the K2 unit is lower than that in the K1 unit. The analysis results indicate that infiltration rates in the K2 unit exhibit a narrower range than those in the K1 and K3 units, suggesting a more uniform infiltration regime. The mean infiltration rate in the K2 unit is lower than that in the K1 unit but slightly higher than that in the K3 unit. Consistent with the steep-slope morphology of the K2 unit, Gan et al. (2023) reported higher soil bulk density and non-capillary porosity, along with lower organic carbon content and soil moisture, in karst areas characterized by increasingly steep slopes and abundant rock outcrops. Several of these conditions have been shown to enhance soil infiltration rates in karst terrains. Based on these findings, the slope morphology of the K2 unit is inferred to contribute to its relatively higher mean infiltration rate compared to the K3 unit.

Conditions of less frequent vegetation density and intensity of agricultural land use reduce the rate of infiltration. This is in line with the conclusion of the Béjar-pulido et al. (2021) which states that the conversion of forest vegetation into agricultural land is negatively correlated with the rate of infiltration. Vegetation on agricultural land has a lower infiltration ability than land under timber trees, which is able to infiltrate water faster through its root network. This statement is reinforced by the conclusion of Hidayat et al. (2024) which states that the root tissue of the plant is able to increase the porosity of the soil. In line with this opinion, The decrease in the infiltration rate in the K2 area corresponds to the decrease in the density of woody vegetation in this area.

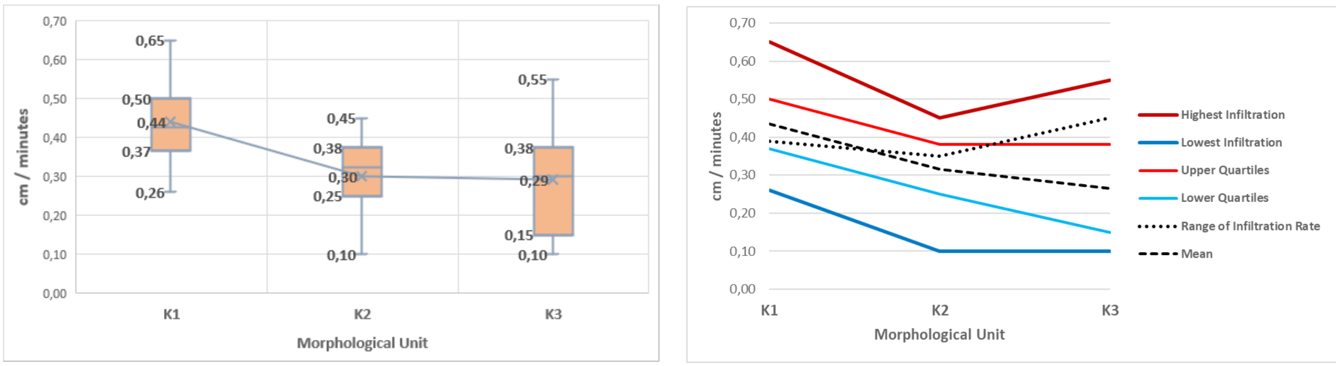

Figure 8. Box-and-whisker graph of infiltration rate data for each morphological unit.
Source: Data calculation

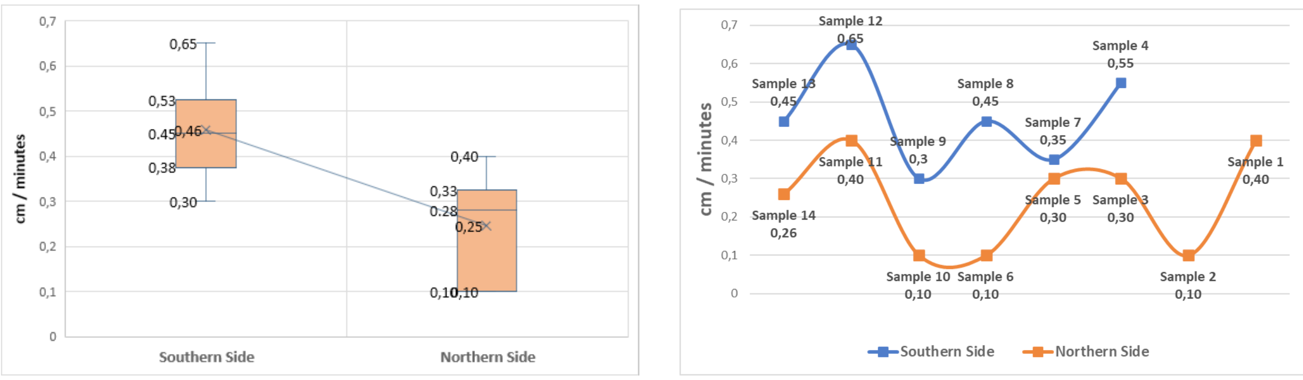

Figure 9. Box-and-whisker graph and infiltration rate patterns of the north and south sides of the Gunungsewu karst area.
Source: data calculation.

The characteristics of the infiltration rate in the K3 morphological unit exhibit notable differences. The K3 area shows a substantially wider range of infiltration-rate values compared with the ranges observed in the K1 and K2 areas. However, the mean, upper quartile, and lower quartile values are lower than those of both K1 and K2. This pattern indicates a greater degree of variability in infiltration behavior within the K3 morphological unit. The highest infiltration rate in this area is 0.55 cm/minute and the lowest is 0.10 cm/minute. These values show almost the same characteristics as the K2 area but have a more complex variation in the level of infiltration than others. The land morphology of this area has a larger flat land with easier access. This condition tends to give rise to more varied land use activities. The morphology of the K3 area is in the form of karst hills that are largely separated by large plains, because the closed karst valley has been largely integrated by intensive dissolution processes (Haryono & Day, 2004). Variations in land use and agricultural forms in karst valleys in the K3 area give rise to varied physical property properties of soil. Wang et al. (2018) concluding that tillage is able to change the macropores and crack networks in karst valley soils resulting in changes in infiltration velocity. Land treatment provides great for changing the type of infiltration by converting preferential infiltration through the gap into matrix infiltration (Liao et al., 2025). The soil in the karst valley of the K3 area is thicker and there are fewer stone insertions on the ground surface than in the K1 and K2 areas. This condition encourages an increase in matrix infiltration which has a lower speed than preferential infiltration (Jiaxin et al., 2025). This condition is indicated by a lower mean infiltration of the K3 area compared to the K1 and K2 areas, but has a wider infiltration velocity range value.

The difference in the characteristics of the level of infiltration speed is also shown spatially based on the classification of the north and south sides of the Gunungsewu karst area. The differences in the characteristics of the infiltration rate of the northern and southern Gunungsewu karst areas are shown in Figure 9.

The box-and-whisker plots illustrate variations in the range of infiltration-rate values, as indicated by differences in the mean, lower quartile, and upper quartile values between the northern and southern sectors. The mean values indicate that infiltration rates on the northern side are lower than those on the southern side. This pattern is further supported by the spatial distribution of infiltration measurements, which shows a clear north–south differentiation across the measurement locations. The infiltration rate at the sample site on the south side ranged from 0.10 cm/minute to 0.4 cm/minute, while the north side ranged from 0.30 cm/minute to 0.65cm/minute. Berdasar analisis pada box-and-whisker graph ditunjukkan nilai mean sisi selatan sebesar 0,46 cm/minute dan sisi utara turun menjadi 0,25 cm/minute.

The results of the analysis of the infiltration rate at the research site showed compatibility with the variation in the distribution of the Gunungsewu karst lithofacies in the north-south direction as outlined by Kusumayudha et al. (1999); Sutoyo (1994), and Tjia (2013). The distribution of the infiltration rate that occurs in the soil has similarities with Gunungsewu karst lithofacies. These findings are in line with (Zhong et al., 2022) which concludes that lithology have significant impact on vegetation and karst soil properties, some of which have a correlation with infiltration capacity in karst area such as bulk density, soil porosity, soil moisture (Gan et al., 2023), soil organic carbon (Lin et al., 2025; Zeng et al., 2024), and soil-rock structure (Jiaxin et al., 2025; Li et al., 2023). Based on this opinion, the difference in karst lithofacies in the research area may be the cause factor for the difference in the characteristics of the infiltration rate on the north and south sides of the Gunungsewu karst. Each infiltration measurement location has cracks in the soil with varying sizes between locations. Voids at the research site were caused by the clay content in the soil as shown by Sunarminto & Santosa (2008). Cracks in the soil at the measurement site are possible to cause preferential flow paths below the surface (Wang et al., 2018). This condition results in an increase in the rate of infiltration in the soil.

4. Conclusion

The characterization of this level of infiltration is carried out as an important step in efforts to protect and preserve the Gunungsewu karst environment. Analysis of the infiltration rate based on morphological units and north-south sides according to lithofacies showed noticeable differences in characteristics. Speeds across the study area ranged from 0.10 cm/min to 0.65 cm/min. The infiltration rate based on morphological units showed that the K1 unit area had the highest infiltration rate, followed by the K2 and K3 unit areas. The mean infiltration of K1 was 0.44 cm/min, K2 was 0.30 cm/min, and K3 was 0.29 cm/min. The K2 unit area has a lower mean value than the K1 unit area and slightly higher than K3, but has the smallest infiltration rate distribution range. The K3 unit area has the lowest mean, but has the largest infiltration value distribution, which shows the most varied infiltration rate variation. The north side of the Gunungsewu karst area has a lower infiltration rate than the south side karst area in both the K1, K2, or K3 unit areas. The infiltration rate of the south side ranges from 0.30 cm/min to 0.65 cm/min, while the north side ranges from 0.10 cm/min to 0.40 cm/min. The spatial distribution of the infiltration rate at the study site showed an increase in the infiltration rate to the west and south. The level of infiltration at the research site is related to the morphological units and lithofacies that underlie the Gunungsewu karst area.

The findings of this study expand the understanding of the characteristics of infiltration rates in karst areas and underlie the development of sustainable karst environmental protection and preservation strategies. Further research needs to focus on practical strategies and methodologies for the protection and sustainable management of karst based on the characteristics of its soil infiltration rate.

Acknowledgement

The authors are grateful to Universitas Negeri Surabaya and Universitas Negeri Yogyakarta for funding this research and publication.

References

Aliyan, S. ., Agusta, V. ., & Bahri, A. . (2023). Analisis Fosil Foraminifera Formasi Wonosari dan Formasi Oyo Pembentuk Morfologi Karst Gunung Sewu Bagian Timur. *Tahun*, *2*(1), 216–226.

Ashgaf, N. M. A., Yoseph, B., & Hendarmawan. (2019). Identifikasi Karakteristik Daerah Infiltrasi Air Tanah berdasarkan Nilai Tekanan Parsial CO2 dan Indeks Kejenuhan CaCO 3 (SIc) di Perbukitan Karst Watuputih. *Jurnal Lingkungan Dan Bencana Geologi*, *10*(2), 27–39.

Bala, J., & Patel, J. (2023). Swelling and Shrinkage Phenomena in Soils. *Futuristic Trends in Agriculture Engineering & Food Sciences Volume 2 Book 9, February*, 339–346. https://doi.org/10.58532/v2bs9ch25

Béjar-pulido, S. J., Cantú-silva, I., & Luna-robles, E. O. (2021). Evaluation and prediction of infiltration in an Andosol under different land uses. *Revista Mexicana de Ciencias Agrícolas*, *12*(7), 1171–1183. https://doi.org/10.29312/remexca.v12i7.2327

BPS. (2025). *Statistik Daerah Istimewa Yogyakarta 2025, Volume 16, Tahun 2025*. BPS Provinsi DIY.

Budiyanto, E., Purnomo, N. H., Muzayanah, Kurniawati, A., Alfaruqi, M., & Syazwana, N. K. (2023). *Karst Valley Land Morphology and Its Uses Patterns in Gunungsewu Karst, Indonesia* (A. Mustofa, I. Widiyanah, B. K. Prahani, I. A. T. Rahayu, M. Mudzakkir, & C. D. M. Putri (eds.); Vol. 785, pp. 1664–1674). Atlantis Press SARL. https://doi.org/10.2991/978-2-38476-152-4_168

Dahak, A., Boutaghane, H., & Merabtene, T. (2022). Parameter Estimation and Assessment of Infiltration Models for Madjez Ressoul Catchment, Algeria. *Water (Switzerland)*, *14*(8), 1–19. https://doi.org/10.3390/w14081185

Elhassan, A. A. M., Mnzool, M., Smaoui, H., Jendoubi, A., Elnaim, B. M. E., & Faihan Alotaibi, M. (2023). Effect of clay mineral content on soil strength parameters. *Alexandria Engineering Journal*, *63*, 475–485. https://doi.org/10.1016/j.aej.2022.08.012

Gan, F., Shi, H., Gou, J., Zhang, L., & Liu, C. (2023). Effects of bedrock strata dip on soil infiltration capacity under different land use types in a karst trough valley of Southwest China. *Catena*, *230*(37), 107253. https://doi.org/10.1016/j.catena.2023.107253

Haryono, E. (2017). Introduction to Gunungsewu Karst: Asian Trans-Disciplinary Karst Conference. *INA-Rxiv*, 0–26.

Haryono, E., & Day, M. (2004). Landform differentiation within the Gunung Kidul Kegelkarst, Java, Indonesia. *Journal of Cave and Karst Studies*, *66*(2), 62–69.

Hervé-Fernández, P., Muñoz-Arriagada, R., Glucevic-Almonacid, C., Bahamonde-Vidal, L., & Radic-Schilling, S. (2023). Influence of Rangeland Land Cover on Infiltration Rates, Field-Saturated Hydraulic Conductivity, and Soil Water Repellency in Southern Patagonia. *Rangeland Ecology and Management*, *90*, 92–100. https://doi.org/10.1016/j.rama.2023.06.004

Hidayat, M., Djufri, D., Basri, H., Ismail, N., Idroes, R., & Ikhwali, M. F. (2024). Influence of vegetation type on infiltration rate and capacity at Ie jue geothermal manifestation, Mount Seulawah Agam, Indonesia. *Heliyon*, *10*(4), e25783. https://doi.org/10.1016/j.heliyon.2024.e25783

Hindersah, R., Firmansyah, Y., & Kurniati, N. (2021). Soil properties of agricultural area in karst terrain of Parakan, Pangandaran, West Java, Indonesia. *Journal of Degraded and Mining Lands Management*, *8*(3), 2809–2814. https://doi.org/10.15243/jdmlm.2021.083.2809

Hu, J., Ci, E., Li, S., Lian, M., & Zhong, S. (2021). *The Pedogenesis of Soil Derived from Carbonate Rocks along a Climosequence in a Subtropical Mountain , China*. 1–22.

Huang, Y., Xiong, T., Zhao, M., Deng, Y., Yang, G., Ban, Y., Lei, T., Yu, X., & Huang, Y. (2024). Influence of soil properties and near-surface roots on soil infiltration process in short-rotation eucalyptus plantations in southern subtropical China. *Catena*, *234*(October 2023), 107606. https://doi.org/10.1016/j.catena.2023.107606

Jiaxin, L., Ziming, D., Liding, C., Huang, Y., & Xiaoyu, P. (2025). Geoderma Quantifying the influence of soil-rock interfaces on water infiltration rate in karst landscapes. *Geoderma*, *460*(June), 117432. https://doi.org/10.1016/j.geoderma.2025.117432

Kusumayudha, S. B., Zen, M. T., Notosiswoyo, S., & Gautama, R. S. (1999). Distribution of the Gunungsewu karstic aquifers based on fractal analysis – case study: Semanu and surrounding area, Yogyakarta, Indonesia. *Bulletin of the Geological Society of*

Malaysia, *43*(August 1998), 345–350. https://doi.org/10.7186/bgsm43199934

Li, B., Shen, L., & Liu, S. (2024). A comparison of soil water infiltration models of moistube irrigation. *Italian Journal of Agronomy*, *19*(1), 100001. https://doi.org/10.4081/ija.2024.2216

Li, H., Zhang, Z., Zhai, J., Yang, L., & Long, H. (2022). Correlation between Soil Structural Parameters and Soil Adhesion Based on Water Film Theory. *Coatings*, *12*(11), 1–14. https://doi.org/10.3390/coatings12111743

Li, X., Contreras, S., Solé-benet, A., Cantón, Y., Domingo, F., Lázaro, R., Lin, H., Wesemael, B. Van, & Puigdefábregas, J. (2011). *Catena Controls of in fi ltration – runoff processes in Mediterranean karst rangelands in SE Spain Vegetation cover rock fragment soil moisture*. *86*, 98–109. https://doi.org/10.1016/j.catena.2011.03.003

Li, X. Y., Contreras, S., Solé-Benet, A., Cantón, Y., Domingo, F., Lázaro, R., Lin, H., Van Wesemael, B., & Puigdefábregas, J. (2011). Controls of infiltration-runoff processes in Mediterranean karst rangelands in SE Spain. *Catena*, *86*(2), 98–109. https://doi.org/10.1016/j.catena.2011.03.003

Li, Y., Wang, S., Peng, T., Zhao, G., & Dai, B. (2023). Hydrological characteristics and available water storage of typical karst soil in SW China under different soil–rock structures. *Geoderma*, *438*(August 2022), 116633. https://doi.org/10.1016/j.geoderma.2023.116633

Liao, Y., Pan, T., Deng, Y., Yang, M., Yang, G., & Yu, X. (2025). Catena Comparing of soil matrix infiltration and preferential flow across different land use types in karst landscapes : Implications for soil and water conservation. *Catena*, *256*(January), 109127. https://doi.org/10.1016/j.catena.2025.109127

Lin, Q., Chen, S., Feng, X., Sounilan, T., & Cheng, K. (2025). Lithological impact on topsoil organic carbon storage of karst forest soils shaped by aggregate pool complexity and their molecular composition. *Applied Soil Ecology*, *206*(July 2024), 105800. https://doi.org/10.1016/j.apsoil.2024.105800

Liu, J., Wu, J., Rong, S., Xiong, Y., & Teng, Y. (2022). Groundwater Vulnerability and Groundwater Contamination Risk in Karst Area of Southwest China. *Sustainability (Switzerland)*, *14*(21), 1–13. https://doi.org/10.3390/su142114483

Luo, D. (2022). The Characteristics of Soil Ca and Mg Leakage in a Karst Depression. *Sustainability (Switzerland)*, *14*(15), 1–12. https://doi.org/10.3390/su14159627

Mulyanto, D., Subroto P.S., S., & Lukito, H. (2011). Genesis Pedon Tanah yang Berkembang di Atas Batuan Karbonat Wonosari Gunungkidul. *Forum Geografi*, *25*(2), 100. https://doi.org/10.23917/forgeo.v25i2.5038

Naufal, M., Adji, T. N., Haryono, E., & Cahyadi, A. (2024). *Assessing karst landscape degradation based on the void development of karst aquifers in Gunungsewu , Indonesia*. *11*(3), 5707–5715. https://doi.org/10.15243/jdmlm.2024.113.5707

Polyakov, V. I., Alekseev, I. I., Orlova, K. S., Abakumov, E. V., & Kostecki, J. (2020). Water holding capacity of Russian Arctic soils (lena river delta and yamal peninsula). *Soil Science Annual*, *71*(1), 37–46. https://doi.org/10.37501/soilsa/121490

Reinhart, H., Putra, R. D., Rafida, M. R., Majiid, M. A., & Maulita, N. S. (2023). Karst of Gunung Sewu Land Use and Land Covers Dynamics: Spatio-Temporal Analysis. *Forum Geografi*, *36*(2), 98–109. https://doi.org/10.23917/forgeo.v36i2.19868

Robin and Bora. (2019). Evaluation of Horton and Modified Kostiakov infiltration model for suitability on hilly slopes. *Indian Journal of Hill Farming December*, *32*(2), 258–264.

Sang, T., Kang, A., Zhang, Y., Li, B., Mao, H., & Kong, H. (2023). Effect of Different Ameliorants on the Infiltration and Decontamination Capacities of Soil. *Materials*, *16*(7). https://doi.org/10.3390/ma16072795

Sari Bahagiarti Kusumayudha, Jatmiko Setiawan, Ayu N. Ciptahening, & Prabawa Dwi Septianta. (2016). Geomorphologic Model of Gunungsewu Karst, Gunung Kidul Regency, Yogyakarta Special Territory, Indonesia: The Role of Lithologic Variation and Geologic Structure. *Journal of Geological Resource and Engineering*, *4*(1), 1–7. https://doi.org/10.17265/2328-2193/2015.01.001

Sitinjak, A. E. S., Rayes, M. L., & Agustina, C. (2019). *MORFOLOGI DAN KLASIFIKASI TANAH PADA BERBAGAI MACAM SUB-LANDFORM KARST DI FORMASI WONOSARI KECAMATAN GEDANGAN , KABUPATEN MALANG Morphology and Classification of Soils on Various Karst Sub-Landform in Wonosari Formation of Gedangan District , Malang Regency*. *6*(1), 1055–1064. https://doi.org/10.21776/ub.jtsl.2019.006.1.4

Srijono, Husein, S., Haryono, E., Yuwono, S. E., Samodra, H., Rachwibowo, P., & Budiadi, E. (2018). Penerapan Pemetaan Geomorfologi Metode ITC dalam Menganalisis Geomorfologi Pegunungan Selatan Jawa Timur. *Prosiding Pertemuan Ilmiah Tahunan Iagi Ke-37 Hotel Horison Bandung*, *M*, 322–336.

Steiakakis, E., Vavadakis, D., & Mourkakou, O. (2023). Groundwater Vulnerability and Delineation of Protection Zones in the Discharge Area of a Karstic Aquifer—Application in Agyia's Karst System (Crete, Greece). *Water*, *15*(2), 231. https://doi.org/10.3390/w15020231

Sunarminto, B. H., & Santosa, H. (2008). *Daya Mengembang dan Mengerut Montmorillonit I : PENGARUH INTENSITAS Curah-embun TERHADAP PENGOLAHAN TANAH Vertisol DI kECAMATAN tEPUS DAN PLAYEN , pegUNUNGAN seribu*. *28*(1), 1–8.

Sunkar, A. (2008). Deforestation and Rocky Desertification Processes in Gunung Sewu Karst Landscape. *Media Konservasi*, *13*(3), 1–7.

Sutoyo. (1994). Sikuen Stratigrsfi Karbonat Gunungsewu. In *Makalah Ikatan Ahli Geologi Indonesia*.

Tjia, H. D. (2013). Morphostructural Development of Gunungsewu Karst , Jawa Island Perkembangan Morfostruktur Kars Gunungsewu di Pulau Jawa. *Indonesian Journal on Geoscience*, *8*(2), 75–88. http://ijog.bgl.esdm.go.id

Tong, K., Guo, J., Chen, S., Yu, F., Li, S., & Dai, Z. (2021). A Simulation Study on the Swelling and Shrinking Behaviors of Nanosized Montmorillonite Based on Monte Carlo and Molecular Dynamics. *Geofluids*, *2021*. https://doi.org/10.1155/2021/1038205

Wang, F., Chen, H., Lian, J., & Fu, Z. (2018). *Preferential Flow in Diferent Soil Architectures of a Small Karst Catchment*. *2001*. https://doi.org/10.2136/vzj2018.05.0107

Widyastuti, M., & Haryono, E. (2016). Water quality characteristics of Jonge Telaga (Doline Pond) as water resources for the people of Semanu District Gunungkidul Regency. *Indonesian Journal of Geography*, *48*(2), 157–167. https://doi.org/10.22146/ijg.17595

Zeng, C., Li, T., He, B., Feng, M., Liang, K., Xu, Q., & Zhao, X. (2024). Catena Vegetation succession increases soil organic carbon density and decreases soil erodibility : Evidence from a karst trough valley experiencing farmland abandonment. *Catena*, *246*(June 2023), 108359. https://doi.org/10.1016/j.catena.2024.108359

Zhang, J., Wang, S., Fu, Z., Chen, H., & Wang, K. (2022). Soil thickness controls the rainfall-runoff relationship at the karst hillslope critical zone in southwest China. *Journal of Hydrology*, *609*(644), 127779. https://doi.org/10.1016/j.jhydrol.2022.127779

Zhang, S., Liu, Y., Yang, M., Tian, P., Mu, X., & Zhao, G. (2025). Impact of vegetation restoration on preferential flow and soil infiltration capacity in the hilly region of the Loess Plateau. *Journal of Hydrology: Regional Studies*, *59*(October 2024), 102333. https://doi.org/10.1016/j.ejrh.2025.102333

Zhang, S., Zhao, G., Fan, J., Yang, M., Tian, P., Mu, X., & Geng, R. (2024). Variations of soil infiltration in response to vegetation restoration and its influencing factors on the Loess Plateau. *Journal of Environmental Management*, *372*(3), 123356. https://doi.org/10.1016/j.jenvman.2024.123356

Zhao, Z., Zhang, H., & Zhang, J. (2025). Catena Impacts of rock-soil interface on soil infiltration and spatio-temporal water distribution during ecosystem succession in karst areas. *Catena*, *260*(115), 109474. https://doi.org/10.1016/j.catena.2025.109474

Zhong, F., Xu, X., Li, Z., Zeng, X., Yi, R., & Luo, W. (2022). Catena Relationships between lithology , topography , soil , and vegetation , and their implications for karst vegetation restoration. *Catena*, *209*(P1), 105831. https://doi.org/10.1016/j.catena.2021.105831

Zou, X., Shekhar, A., Mo, Y., Singh, A. K., Jiang, X., & Liu, W. (2025). Edaphic and climatic effects on soil water dynamics and infiltration patterns in tropical rainforests. *Geoderma*, *455*(January). https://doi.org/10.1016/j.geoderma.2025.117197